2018

Effect Of Resveratrol On The Development Of Eczema

Christopher Carlucci
University of South Carolina

EFFECT OF RESVERATROL ON THE DEVELOPMENT OF ECZEMA

by

Christopher Carlucci

Bachelor of Science
University of South Carolina, 2015

Submitted in Partial Fulfillment of the Requirements

For the Degree of Master of Science in

Biomedical Science

School of Medicine

University of South Carolina

2018

Accepted by:

Carole A. Oskeritzian, Director of Thesis

Sajish Mathew, Reader

Jason L. Kubinak, Reader

Cheryl L Addy, Vice Provost and Dean of the Graduate School

ACKNOWLEDGEMENTS

This study was made possible by the extraordinary support I have received from fellow members of the Mast Cell and Inflammation lab, our collaborators, and my faculty advisers.

Despite my lack of relevant experience, Dr. Carole Oskeritzian welcomed me to her lab with enthusiasm and continues to serve as a model mentor, adviser, and friend. She is a gifted educator and works tirelessly to enable the success of her students.

Alena Chumanevich trained me to perform nearly every procedure used in this study and was always willing to provide any other assistance I needed.

Our doctoral student, Ahmed Aladhami, continues to provide exceptional guidance to every other student the lab. He constantly goes out of his way to explain complex topics, lend a hand, or provide valuable input.

Dr. John Fuseler has invested many hours into imaging and analyzing the histological data presented in this work, on which many of our conclusions are based.

Merlyne Jeanty, Ross Tanis, and Nabihah Kumte have provided regular assistance whenever possible and they are integral to the lab's cohesive dynamic and efficiency.

My thesis committee members, Dr. Jason Kubinak and Dr. Sajish Mathew, have provided extensive guidance throughout this study from its initial design to the publication of my thesis. Dr. Mathew also provided us with the resveratrol used for this study and shared his expert knowledge about the compound.

ABSTRACT

Atopic dermatitis is a type of eczema characterized by chronic inflammation of the skin, affecting millions of people worldwide. Resveratrol, a naturally occurring stilbenoid, is widely believed to exhibit beneficial effects on a host of chronic diseases. Although some previous studies have aimed to evaluate the effects of resveratrol on the pathogenesis of atopic dermatitis, this relationship remains ill-defined. We have previously established that mast cell activation, remodeling, and cellular infiltration in the hypodermis all begin prior to the IgE-mediated immune response in an atopic dermatitis mouse model, and that this early pathogenesis is directly related to an increase in local levels of sphingosine-1-phosphate. We have found novel evidence that treatment with transdermal resveratrol attenuates mast cell activation, perivascular cell infiltration, thickening of the epidermis, and inflammatory chemokines relevant to early-phase atopic dermatitis. We are currently evaluating the effect of resveratrol on local levels of sphingosine-1-phosphate and the activity of sphingosine kinase 1, the major enzyme responsible for its production. The results we have obtained thus far support our hypothesis that resveratrol can attenuate the development of atopic dermatitis, enabling future investigation of its efficacy as a treatment for the disease. We also intend to use these results as a gauge to evaluate the effects of other related compounds on the development of atopic dermatitis.

TABLE OF CONTENTS

Acknowledgements iii

Abstract iv

List of Figures vii

List of Abbreviations viii

Introduction 1

Chapter 1. Methods 4

1.1. Atopic Dermatitis Model 4

1.2. Histology and Microscopy 7

1.3. Morphometric Measurement of Skin Remodeling 8

1.4. Computer Assisted Quantification of Hypodermal Cellular Infiltration 8

1.5. *In situ* Determination of Mast Cell Degranulation 10

1.6. Quantitative Reverse Transcription Polymerase Chain Reaction Assay 10

1.7. Statistics 11

Chapter 2. Results & Discussion 14

2.1. Resveratrol Attenuates Remodeling of the Epidermis During Early-Phase Atopic Dermatitis 14

2.2. Hypodermal Cellular Infiltration is Reduced by Treatment with Resveratrol 16

2.3. Mast Cell Activation is Attenuated by Resveratrol 16

2.4. Treatment with Resveratrol Decreases mRNA Expression of Inflammatory Chemokines 19

Chapter 3. Future Directions 22

3.1. Implications 22

3.2. Ongoing Research 22

3.3. Investigation of the Dose-Response Relationship 24

3.4. Related Compounds 24

3.5. Resveratrol as a Treatment for Atopic Dermatitis 24

References 25

LIST OF FIGURES

Figure 1.1. Morphometric Measurement of Skin Layer Thickness 9

Figure 2.1. Skin Layer Thickness 15

Figure 2.2. Hypodermal Infiltration 17

Figure 2.3. Activity of Mast Cells and Sphingosine Kinase 1 18

Figure 2.4. Chemokine mRNA Expression 21

LIST OF ABBREVIATIONS

AD ..... atopic dermatitis

ANOVA ..... analysis of variance

B2M ß-2-microglobulin

BA ..... ß-actin

BV ..... blood vessel

COX ..... cyclooxygenase

ELISA ..... enzyme-linked immunosorbent assay

ETOH ..... ethanol

FB ..... fiber breadth

H&E ..... hematoxylin and eosin

IgE ..... immunoglobulin E

IOD ..... integrated optical density

MB ..... methylene blue

MC ..... mast cell

NAD^+ ..... nicotinamide adenine dinucleotide

NAM ..... nicotinamide

NR ..... nicotinamide riboside

OR ..... ovalbumin and resveratrol

OV ..... ovalbumin and vehicle

OVA ..... ovalbumin

P ..... probability value

PARP-1 ..... poly ADP-ribose polymerase 1

PR..... perimeter

PTE ..... pterostilbene

qRT-PCR ..... quantitative reverse transcription-polymerase chain reaction

ROI ..... region of interest

RSV ..... resveratrol

S1P sphingosine-1-phosphate

SEM ..... standard error of the mean

SIRT-1 ..... sirtuin-1

SphK1 ..... sphingosine kinase 1

SR..... saline and resveratrol

SV ..... saline and vehicle

TA ..... traced area

TIFF ..... tagged image file format

µg ..... microgram

µL ..... microliter

INTRODUCTION

Resveratrol (RSV) is a naturally occurring stilbenoid most famously found in the skin of grapes. It is widely believed to have a vast array of anti-carcinogenic, anti-inflammatory, and antioxidative protective effects.[1-3] RSV is thought to be responsible for the "French paradox" which is characterized by lower incidence of cardiovascular diseases with red wine consumption, regardless of diets which are typically high in fat.[1] RSV has been shown to modulate different cellular processes including NAD^+ metabolism *via* sirtuin 1 (SIRT-1) and poly ADP-ribose polymerase 1 (PARP-1) pathways, carcinogenesis through the inactivation of cyclooxygenase (COX) proteins, and the phosphorylation of sphingosine by sphingosine kinase 1 (SphK1).[2,4-7] Although these mechanisms have been subject to extensive research over the last two decades, more recent studies have found conflicting evidence surrounding the efficacy of RSV as a treatment in various disease models.[8] One such conflict has arisen from several studies conducted to examine RSV's effects on modulating sphingosine-1-phosphate (S1P), a sphingolipid metabolite with a role in initiating inflammatory responses in mast cells (MC).[5,7,9-11] We suggest this can be explained by variations in experimental design such as routes of administration, dosing, vehicles, specific disease models, and genetic differences in cell-lines and mice used.[12-14] We previously established that S1P is an early modulator of IgE-independent MC activation and skin remodeling in mice, after inducing atopic dermatitis (AD) with ovalbumin (OVA).[9] We used a similar experimental design

for this study to determine the effect of RSV on S1P production and other pre-symptomatic signs of AD pathogenesis.

Multiple studies have shown that RSV can attenuate sphingosine kinase 1 (SphK1)-mediated phosphorylation of sphingosine to produce S1P, but none suggested a specific mechanism of action.[5,7] We hypothesize that RSV prevents translocation of SphK1 from the cytoplasm to the cell membrane, which is required for its activation. We propose that this occurs *via* direct acetylation of SphK1 by RSV in the cytoplasm, based on molecular research done by Dr. Mathew.[6] We anticipate that our pending results will demonstrate inhibition of OVA-induced local skin S1P elevation after transdermal application of RSV, preventing the subsequent changes we have previously characterized during early-phase AD, thus averting progression to disease.[9]

As suggested by previous studies, the low bioavailability of RSV *in vivo* may hinder its delivery in adequate concentrations, limiting its beneficial effects.[12-14] However, other research has shown that delivery of higher RSV concentrations can have adverse pro-inflammatory consequences.[10,11] We have conducted experiments with two different and physiologically relevant concentrations of topical RSV, and though related research is scarce, one study suggests these doses may circumvent both of these limitations.[2]

In addition to providing compelling evidence to support proof of concept, this pilot study has established a standard model so that the results of subsequent research can be accurately compared. In the future, we plan to observe the effect of RSV on the development of AD in the presence of either of two demonstrated cofactors: nicotinamide (NAM) and nicotinamide riboside (NR).[6] We also plan to evaluate another compound

closely related to RSV named pterostilbene (PTE). PTE research is very limited, but some studies have suggested that it may have similar effects with higher bioavailability than RSV.[14-16]

CHAPTER 1. METHODS

1.1. Atopic Dermatitis Model

For all experimental groups in this study, we used a well-established AD mouse model shown to bare similarity to the pathogenesis of AD in humans.[9,17] The methods established by our previous study were adapted to evaluate the development of AD in 8-12 week female wild-type C57Bl/6J mice. Six mice were assigned to each of our four experimental groups using a simple randomization technique as previously reported (see Table 1.1 for group designations).[9]

On Day 1, initial treatment solutions were prepared. First, RSV was dissolved in 100% ethanol (ETOH) to achieve its maximum soluble concentration of 50 mg/mL. This solution was then diluted with 0.9% saline to obtain 2.5 mg RSV/mL 5% ETOH. To obtain final solutions for RSV treated groups, this was either further diluted with 0.9% saline or combined with OVA in 0.9% saline. For vehicle control groups, 5% ETOH was either further diluted with 0.9% saline or combined with OVA in 0.9% saline. All treatment solutions are shown in Table 1.1.

ETOH was used as a vehicle because physiologically relevant concentrations of RSV are insoluble in inorganic solvents such as saline.[2] By first dissolving RSV in ETOH, we were able to maximize its stability and solubility.[14,18] Previous research has suggested that membrane permeability to *trans*-RSV is significantly higher than to *cis*-RSV, and that the *trans*- conformation is only stable once diluted to lower concentrations.[6,13]

Table 1.1. *Experimental Group Designations.*

Group	Day 1 Treatment	Days 2-6 Treatment
Saline and Vehicle (SV)	0.05% ETOH	0.05% ETOH
OVA and Vehicle (OV)	100 µg OVA in 0.05% ETOH	
Saline and RSV (SR)	2.5 µg RSV in 0.05% ETOH	2.5 µg RSV in 0.05% ETOH
OVA and RSV (OR)	100 µg OVA + 2.5 µg RSV in 0.05% ETOH	

For the application of Day 1 treatments, the upper-back areas of mice in each group were shaved then tape-stripped three times. Next, 100 µL of designated treatment solutions were pipetted onto 1 cm by 1 cm square gauze patches. The patches were then applied to the shaved and tape-stripped area of each mouse. A half cm section of sterile flexible tubing was then placed over the patch with one end over the center of the patch and the other extending slightly past its caudal border. The tube and patch were then secured with a Tegaderm transparent dressing so that the patch was completely covered, and the caudal end of the tubing was flush with the edge of the Tegaderm. To ensure that the patch and dressing remained in place, an adhesive bandage was applied over the dressing and 1" of transparent tape was applied to the ends of the bandage.[9] Shaving, tape-stripping, and patching all occurred on Day 1 of the study.

On Days 2-6, all mice received the same treatments without OVA. Treatments given on Days 2-6 are listed in Table 1.1. To apply these daily treatments, Day 1 patches, taped bandages, and Tegaderm dressings were left in place to prevent unintended trauma to the skin. 100 µL of the assigned treatment solution was pipetted through the flexible tubing onto the patch.

On Day 7, mice were euthanized and the patches were removed. A 1 cm by 1 cm skin sample was collected from the treated area and was then cut laterally into four equal strips for histological, mRNA, and lipidomic analyses.[9] All animal procedures were performed in accordance with University of South Carolina Institutional Animal Care and Use Committee approval and all methods used adhere to relevant guidelines and regulations.

1.2. Histology and Microscopy

Skin samples were fixed in 4% fresh paraformaldehyde, paraffin embedded, sectioned, and mounted on microscopy slides by the University of South Carolina School of Medicine's Instrumentation Resource Facility. One slide from each sample was then stained with hematoxylin and eosin (H&E) for measurement of skin layer thickness and determination of cellular infiltration, and another was stained with methylene blue (MB) for MC quantification and MC activation status.

H&E slides were stained by the University of South Carolina School of Medicine's Instrumentation Resource Facility. Tagged image file format (TIFF) images of these slides were obtained using a Nikon E-600 microscope with Micropublisher camera and software at 10x magnification. Cellular infiltration of the hypodermis was quantified using MetaMorph 6.1 software and previously reported morphometric parameters.[9] Skin layer thickness was calculated using the same software and a morphometric measurement technique recently adapted by our lab for this purpose.[21] The investigators who performed this analysis and all subsequent quantifications were single-blinded to slide group designations.

For MB staining, slides were prepared by deparaffinization and rehydration. Slides were then placed in 0.05% MB for five seconds, rinsed with water, dehydrated in 100% ETOH, and mounted under coverslips with cytoseal 60.[9,19] These sections were then imaged using a Nikon E-600 microscope with Micropublisher camera and software to obtain TIFF images at 40x magnification. These images were analyzed with MetaMorph 6.1 software to quantify MCs and detect MC degranulation using morphometric parameters previously published by our lab.[9,20]

1.3. Morphometric Measurement of Skin Remodeling

The epidermal, dermal, and hypodermal thickness of each H&E stained sample was measured using a morphometric measurement technique recently adapted by our lab.[21] Three to six images were obtained per animal at 10x magnification, then three regions of interest (ROI) were randomly selected for each skin layer per image. [9,20] MetaMorph 6.1 software was used to trace the perimeter of the target skin layer in each ROI. The software provided measurements for the traced area (TA) and its perimeter (PR). This TA was treated as an irregular two-dimensional fiber and the equation below was used to calculate the average thickness, or breadth, of each fiber.[21]

$$\text{Fiber Breadth (FB)} = \tfrac{1}{4}\,[PR - (PR^2 - 16TA)^{1/2}]$$

FB measurements were compiled to determine the average thickness of the epidermis, dermis, and hypodermis for each experimental group. This method is depicted in Figure 1.1.

1.4. Computer Assisted Quantification of Hypodermal Cellular Infiltration

To quantify hypodermal cellular infiltration, we used an imaging method previously developed and published by our lab.[9,20] At least 10 images per animal were collected from H&E stained slides and analyzed using MetaMorph 6.1 software. The distinct blue color of hematoxylin-stained nuclei was identified using the hue, saturation, and intensity (HSI) color model through a process called thresholding.[20] To eliminate background, areas that met this color threshold were further analyzed using morphometric parameters to exclude any which were not consistent with previously defined size and shape characteristics of nuclei.[9,20] The software analyzed images using a circular ROI with a fixed diameter (75 μm) which was moved to survey the entire

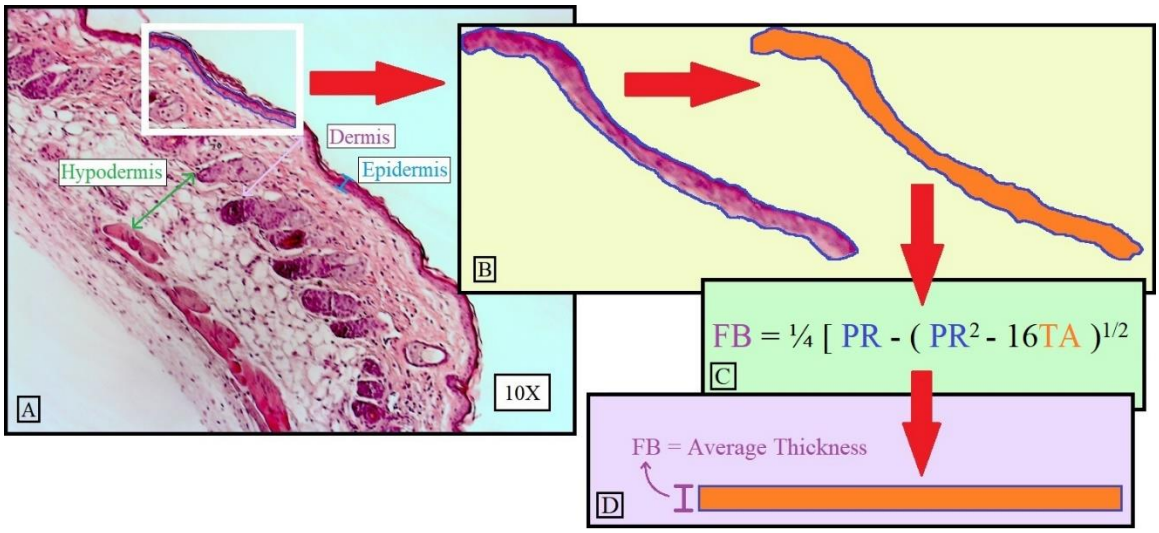

Figure 1.1. *Morphometric Measurement of Skin Layer Thickness.*

[A] is an image obtained from an H&E stained slide at 10x magnification. The portion of the image outlined in white was selected as an ROI for measurement of the epidermis.
[B] represents the tracing and isolation of the epidermis from the ROI depicted in [A] to produce an irregular fiber using MetaMorph software. The software produced values to quantify the TA (orange) in μm^2 and the PR (blue) in µm of the fiber. This representation is enlarged for figure clarity.
[C] displays the equation used to calculate the FB of the fiber shown in [B]. For our purposes, this equation essentially converts the irregular fiber [B] into a rectangle [D] while preserving original length to width ratio.
[D] shows that the FB (purple), or width of the final object represents the average thickness of the epidermis. This method was used to calculate average thickness values for all skin layers.

hypodermis in each image. The software then quantified the number of nuclei present in each ROI and the average number of nuclei per ROI was calculated by group.[9]

1.5. *In situ* Determination of Mast Cell Degranulation

Our lab has previously shown that morphometric parameters can be used to describe the cytoplasm of MCs and define MC activation status.[20] For this analysis, 15 adjacent images of the dermis and hypodermis were recorded as TIFF files from each MB stained slide at 40x magnification. MCs in each image were then identified as individual ROI using the HSI color model thresholding routine of MetaMorph 6.1.[20] HSI values were set to isolate the unique cytoplasmic blue/purple color of MB stained MCs. The software's integrated morphometry routine was then used to measure the area and integrated optical density (IOD) of each thresholded ROI.[20] IOD values represent the total amount of material present in the ROI. The IOD of each ROI was then divided by its area and the resulting values were used to identify whether MCs were intact or degranulated, as previously reported.[9,20] The average number of intact MCs, degranulated MCs, and total MCs present in each experimental group were then calculated, analyzed for significance, and compared.[9]

1.6. Quantitative Reverse Transcription Polymerase Chain Reaction Assay

One strip from each skin sample was designated for analysis by quantitative reverse transcription polymerase chain reaction assay (qRT-PCR). These stripss were snap-frozen immediately after collection and stored at -80°C until RNA extraction. Total RNA was isolated from each sample with the miRNeasy kit from Qiagen using the manufacturer's protocol. The Bioline cDNA synthesis kit and protocol were used to reverse transcribe cDNA from the isolated RNA. QPCR was performed using the Bioline

SYBR No-ROX kit with Bio-Rad CFX Connect equipment and software. We analyzed target gene mRNA expression for chemokines CCL2, CCL3 and CCL5, as well as FcεRIα and SphK1, relative to reference genes ß-2-microglobulin (B2M) and ß-actin (BA). GAPDH was considered as a reference gene but was excluded from data analysis because its expression between samples was less consistent than B2M and BA. All primer sequences are listed in Table 1.2. QPCR conditions were set to the following, as previously reported: 95°C for 10 minutes during the initial step, followed by 40 repeating cycles of 95°C for 10 seconds, annealing at 55°C for 20 seconds, and extension at 72°C for 15 seconds.[9,22] All reactions were performed in duplicate and repeated once. Data was normalized to both reference genes independently and fold-change was determined based on vehicle-control values. A total of eight fold-change values were obtained per animal (48 per experimental group) and outliers were excluded using GraphPad Prism 7.0 software. This software was then used to calculate average fold-change and standard error of the mean (SEM) by group.

1.7. Statistics

For all quantifications, outliers were excluded using GraphPad Prism 7.0 software. This software was then used to perform a one-way analysis of variance (ANOVA) with multiple comparisons to identify statistically significant differences between groups for all quantifications. Differences were considered significant for probability values (P) less than 0.05. GraphPad Prism 7.0 software was used to create all bar graphs. All treatment group results were compared against the SV (vehicle control) group since we have not yet included a true negative control group in this study. All qRT-

Table 1.2. *qRT-PCR Primer Sequences.*

Gene	Forward (F) Reverse (R)	5’ Primer Sequence 3’
B2M	F	CCGAACATACTGAACTGCTACGTAA
	R	CCCGTTCTTCAGCATTTGGA
BA	F	GACGGCCAGGTCATCACTATTG
	R	AGGAAGGCTGGAAAAGAGCC
CCL2	F	CACTCACCTGCTGCTACTCA
	R	GCTTGGTGACAAAAACTACAGC
CCL3	F	GCCATATGGAGCTGACACCC
	R	TAGTCAGGAAAATGACACCTGGC
CCL5	F	TGCCCTCACCATCATCCTCACT
	R	GGCGGTTCCTTCGAGTGACA
FcεRIα	F	ATTGTGAGTGCCACCGTTCA
	R	GCAGCCAATCTTGCGTTACA
SphK1	F	CGTGGACCTCGAGAGTGAGAA
	R	AGGCTTGCTAGGCGAAAGAAG

PCR analyses were performed in duplicate and each experimental group consisted of 6 mice treated in two independent trials. Data collection is not yet complete for some histological analyses and all variations in sample size are clearly reported.

CHAPTER 2. RESULTS & DISCUSSION

2.1. Resveratrol Attenuates Remodeling of the Epidermis During Early-Phase Atopic Dermatitis

Consistent with our previous work with this murine AD model, we found significant thickening of the epidermis and dermis one week after a single exposure to OVA in the group that did not receive treatment with RSV (OV) compared to the vehicle control group (SV).[9] As shown in Figure 2.1A, average thickening of the epidermis was significantly reduced in the group that was exposed to OVA and treated daily with RSV (OR) compared to the OV group. This finding suggests that RSV prevents remodeling of the epidermis during the development of AD.

We have not seen evidence suggesting that RSV has the same ameliorative effect on thickening of the dermis during early-phase AD (Figure 2.1B). However, this may be explained by the fact that we have analyzed six images per animal for measurement of the epidermis, but only three images per animal for the dermis. The cause of this anomaly is not likely to be an inability of RSV to reach the dermis because cellular infiltration of the hypodermis was significantly attenuated after RSV treatment.

Consistent with our previously reported findings, we did not observe any significant thickening of the hypodermis one week after exposure to OVA (Figure 2.1C).[9] Although we did observe significantly increased cellular infiltration in the hypodermis, it does not seem to cause any significant thickening of this skin layer at this early stage of AD pathogenesis.[9] While skin layer thickness is an important indicator of AD, cellular

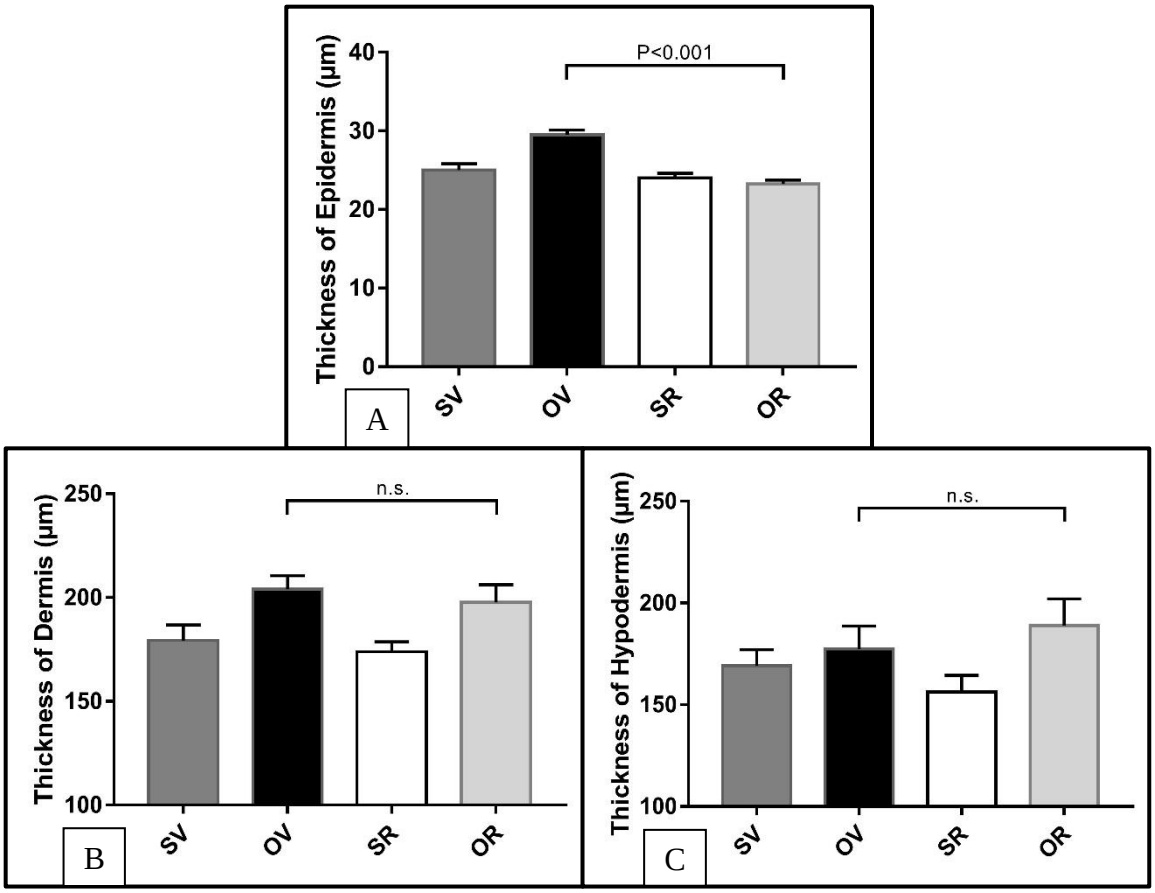

Figure 2.1. *Skin Layer Thickness.*

[A] RSV attenuated OVA-induced thickening of the epidermis. N=3, 6 images per animal, 3 ROI per image. OV>OR, P<0.001. OV>SV, P=0.025. OV>SR, P=0.014. OR=SV, P=0.266. SR=SV, P=0.387. SR=OR, P=0.175.
[B] RSV had no significant effect on OVA-induced thickening of the dermis. N=3, 3 images per animal, 3 ROI per image. OV=OR, P=0.615. OV>SV, P=0.040. OV>SR, P=0.007. OR=SV, P=0.484. SR=SV, P=0.930. SR=OR, P=0.186.
[C] Neither RSV nor OVA exposure had a significant effect on thickening of the hypodermis. N=3, 3 images per animal, 3 ROI per image. OV=OR, P=0.859. OV=SV, P=0.939. OV=SR, P=0.462. OR=SV, P=0.527. SR=SV, P=0.811. SR=OR, P=0.119.

infiltration of the hypodermis likely begins before thickening of any skin layer can be detected.

2.2. Hypodermal Cellular Infiltration is Reduced by Treatment with Resveratrol

Using morphometric parameters we have previously defined, we were able to quantify cellular infiltration of the entire area of the hypodermis mounted on each H&E stained slide.[9,20] The number of nuclei identified in each ROI were compiled according to experimental group designation and group averages were compared. A separate quantification of the number of nuclei present in each ROI which contained blood vessels (BV) was also performed and data from both quantifications of hypodermal cellular infiltration is displayed in Figure 2.2.

As we observed previously, both whole hypodermal and perivascular cellular infiltration were significantly increased one week after a single exposure to OVA.[9] The magnitude of this OVA-induced cellular infiltration was significantly decreased after daily treatment with RSV, both in the whole hypodermis and near hypodermal blood vessels specifically. These findings indicate that RSV can prevent the development of AD by reducing the recruitment of cells likely to contribute to early inflammation and tissue remodeling. Although these significant increases in hypodermal cellular infiltration for OVA exposed groups is significant, hypodermal thickening may not be observed until longer-term effects of this infiltration occur.

2.3. Mast Cell Activation is Attenuated by Resveratrol

We used our previously described morphometric method to determine the average total number of MCs, intact MCs, and degranulated (or activated) MCs per mm^2 of skin tissue for each treatment group. As shown in Figure 2.3A, we did not observe any

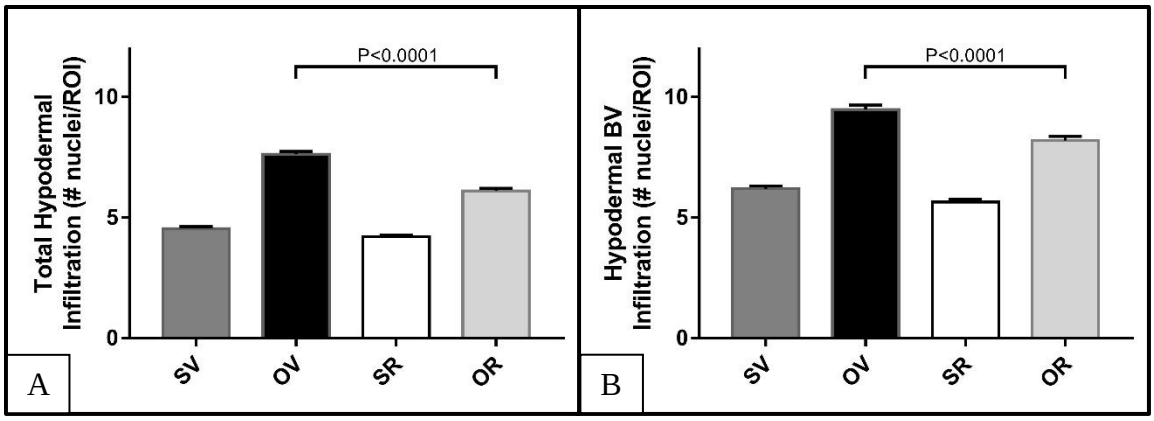

Figure 2.2. *Hypodermal Infiltration.*

[A] RSV significantly decreased OVA-induced cellular infiltration in the whole hypodermis. N=6, 10 images per animal, 10 ROI per image, 600 ROI per group. OV>OR, P<0.0001. OV>SV, P<0.0001. OV>SR, P<0.0001. OR>SV, P<0.0001. SR=SV, P=0.0713. OR>SR, P<0.0001.
[B] RSV significantly decreased OVA-induced cellular infiltration around BV in the hypodermis. N=6, 10 images per animal, only ROI from [A] containing BV included, 225-255 ROI per group. OV>OR, P<0.0001. OV>SV, P<0.0001. OV>SR, P<0.0001. OR>SV, P<0.0001. SR=SV, P=0.0804. OR>SR, P<0.0001.

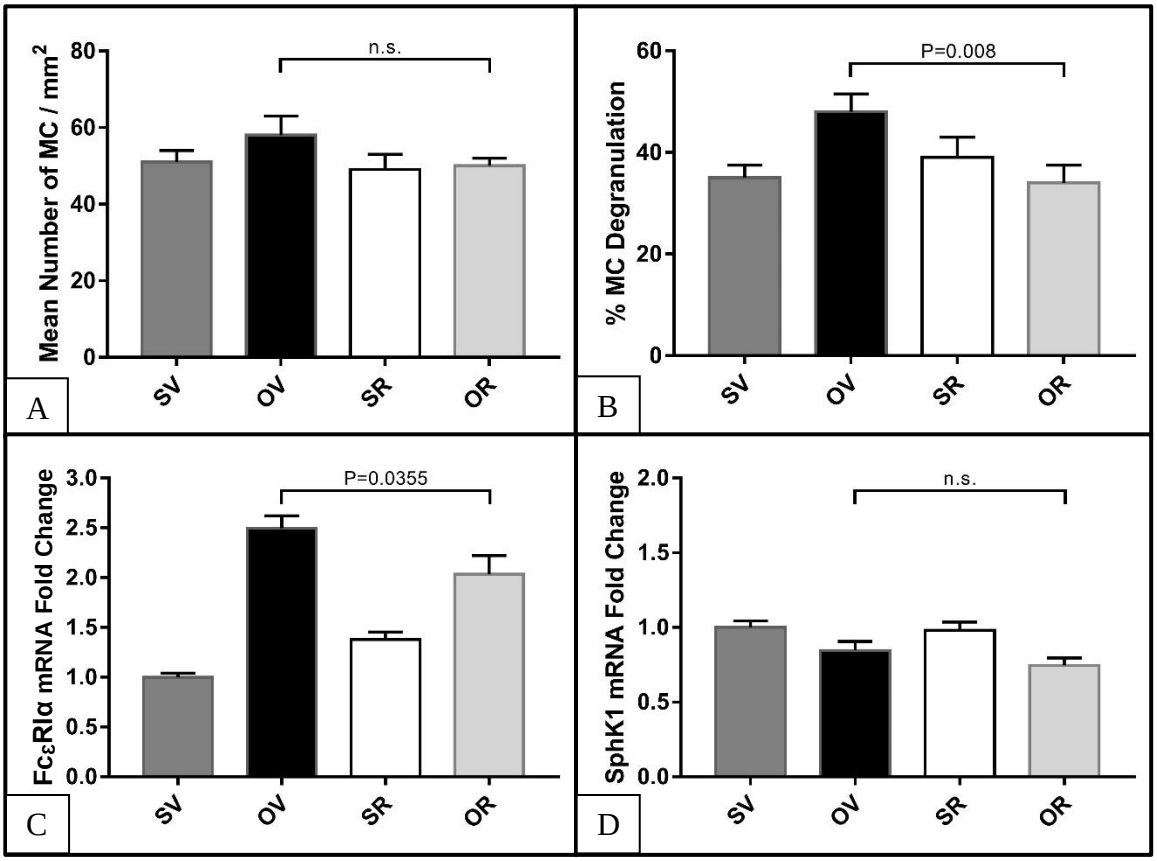

Figure 2.3. *Activity of Mast Cells and Sphingosine Kinase 1.*

[A] Neither OVA exposure nor treatment with RSV had a significant effect on the mean number of all MCs. N=3, 15 images per animal. OV=OR, P=0.281. OV=SV, P=0.342. OV=SR, P=0.145. OR=SV, P=0.561. SR=SV, P=0.263. OR=SR, P=0.344.
[B] RSV prevented OVA-induced MC degranulation. N=3, 15 images per animal. OV>OR, P=0.008. OV>SV, P=0.033. OV=SR, P=0.251. OR=SV, P=0.875. SR=SV, P=0.734. OR=SR, P=0.371.
[C] RSV significantly decreased OVA-induced upregulation of FcεRIα mRNA. N=6, 8 fold-change values calculated per animal, 48 fold-change values per group. OV>OR, P=0.0355. OV>SV, P<0.0001. OV>SR, P<0.0001. OR>SV, P<0.0001. SR=SV, P=0.1098. OR>SR, P=0.0009.
[D] Neither OVA exposure nor treatment with RSV had a significant effect on SphK1 mRNA expression. N=6, 8 fold-change values calculated per animal, 48 fold-change values per group. OV=OR, P=0.5364. OV=SV, P=0.1621. OV=SR, P=0.2709. OR<SV, P=0.0041. SR=SV, P=0.9929. OR<SR, P=0.0100.

significant differences in the average number of MCs per mm^2 between groups. However, Figure 2.3B demonstrates significantly increased MC degranulation one week after exposure to OVA and that this increase in degranulation was attenuated after RSV treatment.

As shown in Figure 2.3C, FcεRIα mRNA expression was significantly increased one week after OVA exposure and this increase was ameliorated after treatment with RSV. FcεRIα is the alpha chain of the high affinity IgE receptor. FcεRIα expression in the skin is effectively exclusive to MCs and we have previously shown that its relative mRNA expression correlates to the local abundance of MCs.[9,24] It is possible that RSV decreases expression of FcεRIα by MCs, making them less susceptible to IgE-mediated activation. However, further work is needed to reconcile the discrepancies between this data and the results of our histological quantification of MCs.

Figure 2.3D shows that we found no significant differences in SphK1 mRNA expression between groups. This result neither supports nor weakens our hypothesis that RSV reduces the activity of SphK1. Since we suggest RSV works by preventing the translocation of SphK1 to the cell membrane to reach its substrate, its mRNA expression may not be affected.

2.4. Treatment with Resveratrol Decreases mRNA Expression of Inflammatory Chemokines

We have previously shown that CCL2, CCL3 and CCL5 are significant contributors to allergic airway and AD skin inflammation.[9,24] Based on our previous research, we know that OVA exposure promotes the expression of these chemokines.[9] The results of our current work are consistent with our previous findings, except that we found no significant increase in CCL3 mRNA expression after OVA exposure. However,

this previously reported increase was significantly less than the increases observed in CCL2 and CCL5 mRNA. In support of our hypothesis, we have found that mRNA expression for both CCL2 and CCL5 were significantly decreased in the OVA exposed group that was treated with RSV, compared to the OVA exposed group that did not receive treatment. This is consistent with the RSV-mediated decrease in hypodermal cellular infiltration we observed because these chemokines are responsible for immune cell recruitment. This data is displayed in Figure 2.4.

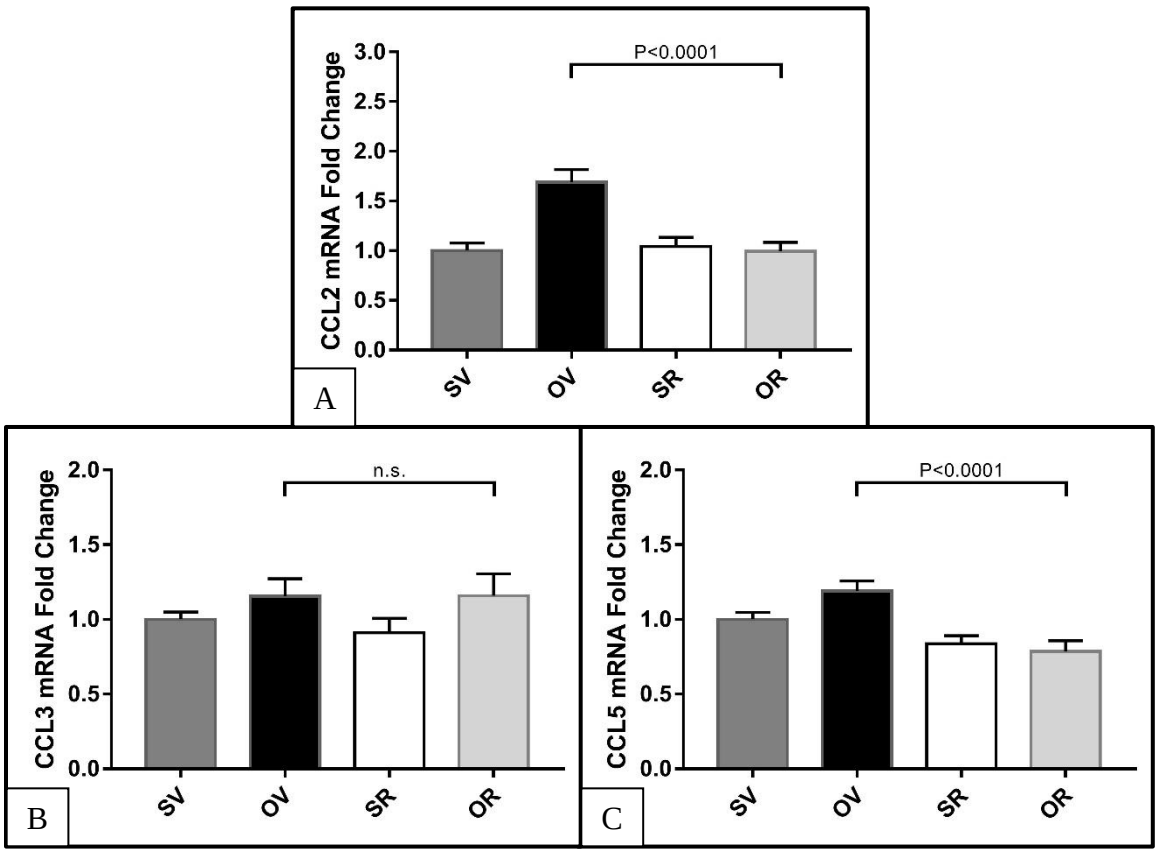

Figure 2.4. *Chemokine mRNA Expression.*

[A] RSV prevented OVA-induced upregulation of CCL2 mRNA expression. N=6, 8 fold-change values calculated per animal, 48 fold-change values per group. OV>OR, P<0.0001. OV>SV, P<0.0001. OV>SR, P<0.0001. OR=SV, P>0.9999. SR=SV, P=0.9910. OR=SR, P=0.9883.
[B] Neither OVA exposure nor treatment with RSV caused a significant change in the mRNA expression of CCL3. N=6, 8 fold-change values calculated per animal, 48 fold-change values per group. OV=OR, P>0.9999. OV=SV, P=0.7346. OV=SR, P=0.4175. OR=SV, P=0.7225. SR=SV, P=0.9439. OR=SR, P=0.4060.
[C] RSV prevented OVA-induced upregulation of CCL5 mRNA expression. N=6, 8 fold-change values calculated per animal, 48 fold-change values per group. OV>OR, P<0.0001. OV>SV, P=0.0123. OV>SR, P=0.0003. OR=SV, P=0.0604. SR=SV, P=0.2252. OR=SR, P=0.9312.

CHAPTER 3. FUTURE DIRECTIONS

3.1. Implications

The goals of this pilot study were to determine if topical application of RSV: 1) has any effect on early IgE independent S1P elevation, MC activation, chemokine expression, cellular infiltration, as well as remodeling of skin tissue, and 2) affects the translocation of SphK1 to the cell membrane to reach its substrate. While this study is not yet complete, we now have enough evidence to conclude that topical application of RSV may serve as a prophylactic agent for AD. This conclusion serves as proof of our concept, enabling us to proceed with related work in the future. We intend to use our findings as standards for the evaluation of our upcoming research into effects of alternative dosing, similar compounds, and RSV as a treatment for AD.

3.2. Ongoing Research

Although we have already found evidence to support several elements of our hypothesis, we are still working to complete the picture. Our outstanding objectives include determining: 1) how the effects of a lower dose of RSV differ from the dose we have already investigated, 2) whether RSV attenuates the enzymatic activity of SphK1 by preventing its translocation to the cell membrane, 3) if RSV affects local S1P levels, and 4) if our ETOH vehicle causes any effects.

We have already completed another group of trials using a lower dose of RSV (1 μg), but we have not yet been able to perform data analysis of these samples. Once we compare these results to those observed for the 2.5 μg treatment group, we will know if we should evaluate higher or lower doses in future trials.

We are also currently working on localizing SphK1 at the subcellular level which will allow us to determine if RSV alters the translocation of SphK1 to the cell membrane, preventing it from reaching its substrate. Subcellular localization of SphK1 will be accomplished by staining of slides with immunofluorescent antibodies and collecting images *via* confocal microscopy. Slides will be deparaffinized and rehydrated before heat induced antigen retrieval. Phalloidin conjugated with AlexaFuor™ (488 nm) will be used for actin staining. Slides will then be treated with a rabbit anti-mouse anti-SphK1 antibody or an isotype-matched negative control antibody. We will then use a goat anti-rabbit Cy™ 3 (543nm) secondary antibody and mount slides using the VECTASHIELD™ DAPI paramount medium. A confocal microscope and software will be used to collect images to determine the cytoplasmic and membrane associated distributions of SphK1. We anticipate that there will be more membrane associated SphK1 in the MCs of animals exposed to OVA compared to vehicle controls, and that this increase is attenuated by RSV treatment.

To strengthen our current results, we also plan to quantify local S1P *via* tissue lipidomic analysis to determine whether this mediator of the early inflammatory response is affected by RSV treatment. Tissue samples will be sent to the VCU Lipidomics Core for analysis using liquid chromatography-electrospray ionization-tandem mass

spectrometry, as previously reported.[9] S1P quantities will be normalized to sample weight, averaged by group, and analyzed for significant differences.

Prior to completing this pilot study, we will also perform another trial to ensure that our ETOH vehicle does not have any unanticipated effects. This trial will be performed using the previously described methods and will consist of a vehicle only group, a vehicle and OVA group, a saline only group, and a saline and OVA group.

3.3. Investigation of the Dose-Response Relationship

As previously stated, the doses chosen for our initial evaluation of RSV were selected based on their theorized biological relevance and limited related research. In addition to these 2.5 µg and 1.0 µg doses, we plan to evaluate the effects of doses that are either higher or lower depending on the results of our 1.0 µg trial to obtain a clearer picture of RSV's dose-response curve.

3.4. Related Compounds

Due to scarce research into resveratrol and pterostilbene alone or in combination with NAM and NR cofactors with respect to chronic inflammatory diseases, this initial study provided us with the data we will need to determine if these other compounds can be at least as effective as resveratrol in the prevention of AD.

3.5. Resveratrol as a Treatment for Atopic Dermatitis

Since we have found that resveratrol can ameliorate several important effector mechanisms of AD pathogenesis, we will investigate whether it can reverse AD-associated changes once they have already occurred using the same murine AD model.

REFERENCES

1. Frémont L Minireview – biological effects of resveratrol. *Life Sciences*. 2000;66: 663–673.

2. Jang M, Cai L, Udeani GO, Slowing KV, Thomas CF, Beecher CW, Fong HH, Farnsworth NR, Kinghorn AD, Mehta RG, Moon RC, Pezzuto JM. Cancer chemopreventive activity of resveratrol, a natural product derived from grapes. *Science*. 1997 Jan 10;275(5297):218-220.

3. Pan Y, Zhang H, Zheng Y, Zhou J, Yuan J, Yu Y, Wang J. Resveratrol Exerts Antioxidant Effects by Activating SIRT2 To Deacetylate Prx1. *Biochemistry*. 2017 Dec 5;56(48):6325-6328.

4. Sajish M, Zhou Q, Kishi S, Valdez DM Jr, Kapoor M, Guo M, Lee S, Kim S, Yang XL, Schimmel P. Trp-tRNA synthetase bridges DNA-PKcs to PARP-1 to link IFN-γ and p53 signaling. *Nature Chemical Biology*. 2012 Apr 15;8(6):547-554.

5. Lim KG, Gray AI, Pyne S, Pyne NJ. Resveratrol dimers are novel sphingosine kinase 1 inhibitors and affect sphingosine kinase 1 expression and cancer cell growth and survival. *British Journal of Pharmacology*. 2012 Jul;166(5):1605-1616.

6. Sajish M, Schimmel P. A human tRNA synthetase is a potent PARP1-activating effector target for resveratrol. *Nature*. 2015 Mar 19;519(7543):370-373.

7. Brizuela L, Dayon A, Doumerc N, Ader I, Golzio M, Izard JC, Hara Y, Malavaud B, Cuvillier O. The sphingosine kinase-1 survival pathway is a molecular target for the tumor-suppressive tea and wine polyphenols in prostate cancer. *FASEB Journal*. 2010 Oct;24(10):3882-3894.

8. Berman AY, Motechin RA, Wiesenfeld MY, Holz MK. The therapeutic potential of resveratrol: a review of clinical trials. *NPJ Precision Oncology*. 2017;1.

9. Wedman PA, Aladhami A, Chumanevich AP, Fuseler JW, Oskeritzian CA. Mast cells and sphingosine-1-phosphate underlie prelesional remodeling in a mouse model of eczema. *Allergy*. 2018 Feb;73(2):405-415.

10. Kurano M, Hara M, Nojiri T, Ikeda H, Tsukamoto K, Yatomi Y. Resveratrol exerts a biphasic effect on apolipoprotein M. *British Journal of Pharmacology*. 2016 Jan;173(1):222-233.

11. Park K, Elias PM, Hupe M, Borkowski AW, Gallo RL, Shin KO, Lee YM, Holleran WM, Uchida Y. Resveratrol stimulates sphingosine-1-phosphate signaling of cathelicidin production. *Journal of Investigative Dermatology*. 2013 Aug;133(8):1942-1949.

12. Smoliga, J.M.; Colombo, E.S.; Campen, M.J. A healthier approach to clinical trials evaluating resveratrol for primary prevention of age-related diseases in healthy populations. *Aging*. 2013;5:495–506.

13. Smoliga JM, Blanchard O. Enhancing the delivery of resveratrol in humans: if low bioavailability is the problem, what is the solution? *Molecules*. 2014 Oct 24;19(11):17154-17172.

14. Robinson, K., Mock, C., & Liang, D. Pre-formulation studies of resveratrol. *Drug Development and Industrial Pharmacy*. 2015;*41*(9):1464–1469.

15. Zhang L, Wen X, Li M, Li S, Zhao H. Targeting cancer stem cells and signaling pathways by resveratrol and pterostilbene. *Biofactors*. 2017 Dec 4.

16. Lange KW, Li S. Resveratrol, pterostilbene, and dementia. *Biofactors*. 2017 Nov 23.

17. Speigel JM, Mizoguchi E, Brewer JP, Martin TR, Bhan AK, Geha RS. Epicutaneous sensitization with protein antigen induces localized allergic dermatitis and hyperresponsiveness to methacholine after single exposure to aerosolized antigen in mice. *Journal of Clinical Investigation*. 1998;101:1614-1622.

18. Xilan S, Bin P, Weidong Y. Measurement and correlation of solubility of trans-resveratrol in 11 solvents at T=(278.2, 288.2, 298.2, 308.2, and 318.2)K. *Journal of Chemical Thermodynamics*. 2008;40(4):735-738.

19. Wolters PJ, Mallen-St Clair J, Lewis CC, *et al.* Tissue-selective mast cell reconstitution and differential lung gene expression in mast cell deficient Kit (W-sh)/Kit(W-sh) sash mice. *Clinical and Experimental Allergy*. 2005;35:82-88.

20. Wedman P, Aladhami A, Beste M, *et al.* A new image analysis method based on morphometric and fractal parameters for rapid evaluation of in situ mammalian mast cell status. *Microscopy and Microanalysis.* 2015;21:1573-1581.

21. Russ JC. The Image Processing Handbook. 6. Boca Raton: CRC Press; 2011.

22. Chumanevich AP, Wedman PA, Oskeritzian CA. Methods for Analyzing Sphingosine-1-Phosphate Signaling in Human and Mouse Primary Mast Cells. Methods Mol Biol. 2018;1697:21-30.

23. Hait NC, Allegood J, Maceyka M, *et al.* Regulation of histone acetylation in the nucleus by sphingosine-1-phosphate. *Science*. 2009;325:1254-1257.

24. Oskeritzian CA, Hait NC, Wedman P, *et al*. The sphingosine-1-phosphate/ sphingosine-1-phosphate receptor 2 axis regulates early airway T-cell infiltration in murine mast cell-dependent acute allergic responses. *Journal of Allergy and Clinical Immunology*. 2015;135:1008-1018.